Taylor & Francis
Taylor & Francis Group

Vehicle System Dynamics
International Journal of Vehicle Mechanics and Mobility

ISSN: 0042-3114 (Print) 1744-5159 (Online) Journal homepage: https://www.tandfonline.com/loi/nvsd20

Autonomous collision avoidance system by combined control of steering and braking using geometrically optimised vehicular trajectory

Ryuzo Hayashi , Juzo Isogai , Pongsathorn Raksincharoensak & Masao Nagai

To cite this article: Ryuzo Hayashi , Juzo Isogai , Pongsathorn Raksincharoensak & Masao Nagai (2012) Autonomous collision avoidance system by combined control of steering and braking using geometrically optimised vehicular trajectory, Vehicle System Dynamics, 50:sup1, 151-168, DOI: 10.1080/00423114.2012.672748

To link to this article: https://doi.org/10.1080/00423114.2012.672748

Vehicle System Dynamics
Vol. 50, Supplement, 2012, 151–168

Taylor & Francis
Taylor & Francis Group

Autonomous collision avoidance system by combined control of steering and braking using geometrically optimised vehicular trajectory

Ryuzo Hayashi*, Juzo Isogai, Pongsathorn Raksincharoensak and Masao Nagai

Department of Mechanical Systems Engineering, Tokyo University of Agriculture and Technology, 2-24-16 Naka-cho Koganei, Tokyo 184-8588, Japan

(*Received 21 October 2011; final version received 1 March 2012*)

This study proposes an autonomous obstacle avoidance system not only by braking but also by steering, as one of the active safety technologies to prevent traffic accidents. The proposed system prevents the vehicle from colliding with a moving obstacle like a pedestrian jumping out from the roadside. In the proposed system, to avoid the predicted colliding position based on constant-velocity obstacle motion assumption, the avoidance trajectory is derived as connected two identical arcs. The system then controls the vehicle autonomously by the combined control of the braking and steering systems. In this paper, the proposed system is examined by real car experiments and its effectiveness is shown from the results of the experiments.

Keywords: active safety, collision avoidance systems, driver assistance systems, autonomous vehicles, evasive steering

1. Introduction

In recent years, the development of collision safety technologies has had an effect on a remarkable decrease in traffic fatalities; however, the number of road accidents remains high. Therefore, preventive safety technologies are expected to reduce the number of accidents. Although some technologies such as ABS and DYC are contributing to accident prevention, they are still not enough to completely eliminate the traffic accidents. Due to a delayed recognition or a judgement error, approximately 40% of drivers do not take any avoidance manoeuvre at the time of a traffic accident [1,2]. Therefore, to reduce accidents caused by these human errors, it is desirable that the vehicles are able recognise their surroundings and take appropriate avoidance manoeuvres when necessary. Some autonomous collision avoidance systems, which use emergency braking, have been launched in the automobile market and their functionality as 'Crash-Free Vehicles' has attracted automotive users and many engineers.

*Corresponding author. Email: ryuzoh@cc.tuat.ac.jp

ISSN 0042-3114 print/ISSN 1744-5159 online

http://dx.doi.org/10.1080/00423114.2012.672748
http://www.tandfonline.com

In addition to braking, evasive steering can be an alternative way to avoid collisions with frontal obstacles. Treating the vehicle as a point mass model, the limit of time-to-collision (TTC) in which a collision can be avoided by steering is constant with running speed [3]. It has also been reported that in general, evasive steering is more effective in forward obstacle avoidance versus braking when driving at higher speed [4]. Conversely, an autonomous collision avoidance system by steering has not been put into practice as it is still in the research and development stage. This is due to the difficulties of recognising the surroundings properly and formulating a steering manoeuvre assuring safe evasion of an obstacle.

Examples of research on emergency avoidance by steering include: The vehicle motion control method which minimises the collision risk value proposed by Fujioka *et al.* [5] and that which minimises the resultant force proposed by Ohmuro *et al*. [6]. These researchers mainly utilise complex control theories. In contrast, the authors have proposed a geometrical optimisation method of avoidance trajectory [7]. The proposed method is reasonable from a practical viewpoint because the availability of avoidance can be judged before starting avoidance manoeuvre and the computational cost is low. However, applicable conditions of these theories are limited in specific circumstances that the obstacles to avoid are stationary and do not consider moving obstacles shifting into the ego-vehicle's path.

Based on the aforementioned, this paper proposes an autonomous avoidance system of moving obstacles as one of the collision avoidance technologies by steering. Based on motion prediction of the obstacle, the proposed system is designed to take appropriate evasive action autonomously from moving obstacles. The effectiveness of the designed system is examined by demonstration experiments.

2. Target scenario and the experimental vehicle

2.1. *Target scenario*

This paper focuses on the following scenario: While the ego-vehicle is driven with road boundaries on both sides, a frontal obstacle jumps out from the roadside. In order to simplify the derivation of the avoidance trajectory, this paper supposes the following conditions, as illustrated in Figure 1.

(1) The road is straight with road boundaries on both sides in an urban area.
(2) Only a single obstacle appears from the roadside when the ego-vehicle is in motion.
(3) It is impossible to avoid the obstacle by evading leftward due to a small clearance between the obstacle and the left-side road boundary.
(4) There is an enough space between the obstacle and the right-side road boundary for the vehicle to pass through.

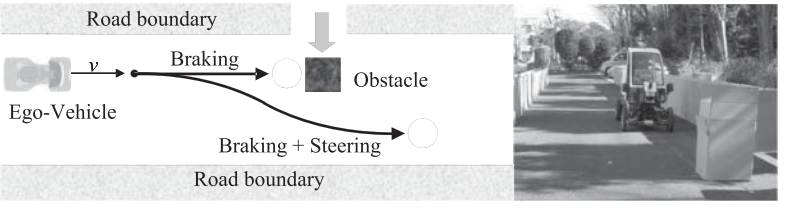

Figure 1. Target scenario.

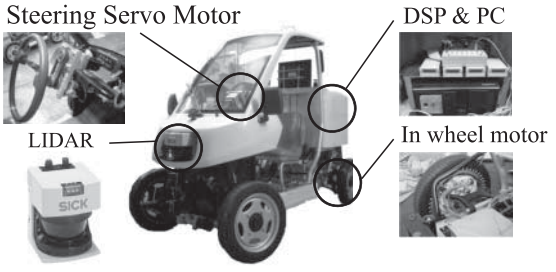

Figure 2. The experimental vehicle.

Concerning the motion of the obstacle, the following conditions are assumed:

(5) Regardless of vehicle avoidance action, the obstacle continues moving perpendicularly to the road at a constant speed.
(6) The speed of the obstacle is approximately 1 m/s, which is the same speed as a typical pedestrian.

Concerning the ego-vehicle, the following condition is assumed:

(7) The ego-vehicle's speed is under 30 km/h, since the road is an urban street.

2.2. *Experimental vehicle*

The experimental vehicle in this research is shown in Figure 2. The vehicle is equipped with a laser range finder (LIDAR: Light Imaging Detection and Ranging) at the front and is able to obtain the relative distances to objects over a wide range. It is also equipped with ordinary vehicle motion sensors such as accelerometers, a vehicle speed sensor and a yaw rate sensor. In addition, a digital signal processor is installed on the vehicle to control the vehicle velocity and steering angle by means of in-wheel motors and an AC-servo motor, respectively.

3. Theory

This section describes the collision avoidance methods proposed in the authors' previous study [7]. They are utilised in the autonomous collision avoidance system designed in Section 4.

In this theory, the dynamics of the vehicle and the steering system are not considered in order to simplify the theoretical equations. The vehicle is assumed to be able to instantly realise turning in any radius as long as the radius is larger than the minimum turning radius of the vehicle. This means that an actual vehicle cannot execute the theory rigorously. However, since this avoidance system is supposed to be utilised in urban areas whose speed limit is 30 km/h, the influence of the dynamics is negligible and can be compensated by additionally estimating an extra margin to the obstacle.

3.1. *Avoidance by braking*

This is an avoidance method by braking without any steering manoeuvre. This can be subdivided into the following two types.

3.1.1. *Braking A*

Braking A is defined as a collision avoidance method that makes the ego-vehicle decelerate with maximum deceleration a_x by braking to stop before the obstacle. Since it is conducted without any steering, the vehicle trajectory is a simple straight line along the direction of the ego-vehicle.

3.1.2. *Braking B*

Even though the ego-vehicle cannot stop before the obstacle, there is a possibility to avoid collision by braking without steering, because braking delays the arrival time of the ego-vehicle to the obstacle. The moving obstacle may pass through the ego-vehicle's path due to this delay. Braking B is defined as a collision avoidance method by letting the obstacle finish crossing the ego-vehicle's path by braking with maximum deceleration a_x. The vehicle trajectory of Braking B is a simple straight line along the direction of the ego-vehicle.

3.2. *Avoidance by evasive steering*

The avoidance by evasive steering method drives the ego-vehicle along a trajectory where the vehicle avoids the obstacle and the road boundary by conducting appropriate steering manoeuvres with braking. In this study, since the lateral acceleration is constant in steady-state cornering, the desired evasive trajectory is formulated as connected twin arcs in order to minimise the steady lateral acceleration during the evasive motion. Therefore, the avoidance trajectory is derived geometrically as twin arcs which have as large a radius as possible within the range to avoid a collision with the obstacle and the road boundary. In addition, the ego-vehicle is made to decelerate with maximum deceleration a_x to stop as soon as possible after the evasive action. Avoidance by evasive steering can be subdivided into two types as listed below:

3.2.1. *Steering A*

This avoidance method is for cases in which the position of a right road boundary does not need to be taken into account because the right road boundary is far enough from the ego-vehicle. Figure 3(a) shows the conceptual image of the formulation and the descriptions of the symbols.

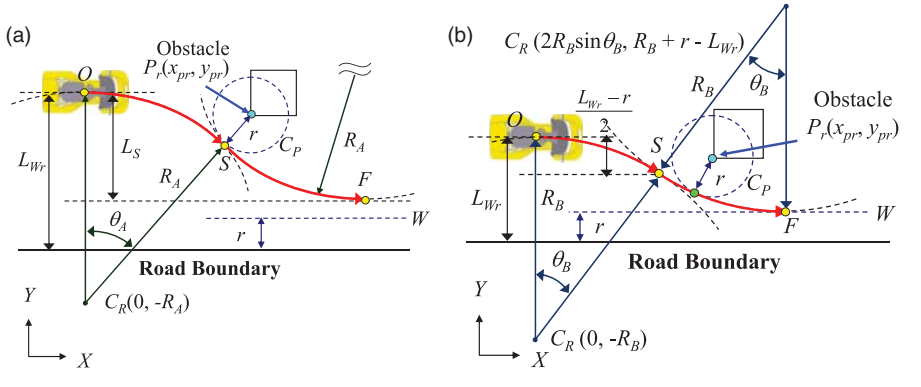

Figure 3. Geometric derivation of avoidance trajectory. (a) Steering A and (b) Steering B.

To begin with, the circle C_P is drawn centred on the right edge of the obstacle with radius r, which means the half width of the ego-vehicle. Second, the circle C_R is drawn so that it is circumscribed to the circle C_P and its tangent line at point O is in the same direction as the travelling direction of the ego-vehicle. This circle C_R is the largest circle with which the ego-vehicle can avoid collision with the obstacle. Here, the tangent point of C_R with C_P is termed as the steering switching point S.

Next, the other circle with the same radius as C_R is drawn so that the circle C_P is inscribed in it at the point S. The finishing point F is defined where the length of the arc OS equals to that of the arc OF. Thus, the desired avoidance trajectory is drawn as the curve OSF.

In this condition, the following equation must be satisfied because the circle C_R is circumscribed to the circle C_P:

$$R_A + r = \sqrt{x_{pr}^2 + (R_A + y_{pr})^2}. \tag{1}$$

Hence, the turning radius R_A is obtained as follows:

$$R_A = \frac{x_{pr}^2 + y_{pr}^2 - r^2}{2(r - y_{pr})}. \tag{2}$$

Regarding the turning angle θ_A, the following equation must be satisfied:

$$(R_A + r)\cos\theta_A = R_A + y_{pr}. \tag{3}$$

As a result, the turning angle θ_A is obtained dependent on the turning radius R_A as follows:

$$\theta_A = \cos^{-1}\left(\frac{R_A + y_{pr}}{R_A + r}\right). \tag{4}$$

Thus, the turning radius and turning angle of Steering A can be determined by Equations (2) and (4).

3.2.2. *Steering B*

This avoidance method is for cases where the presence of the right road boundary must be taken into account because the ego-vehicle may collide with the road boundary with Steering A. Figure 3(b) shows the conceptual image of the formulation and the descriptions of the symbols.

In this case, target line W is first drawn r away from the right road boundary. At the same time, circle C_P is drawn. Then the point where the latter circle C'_R is tangent to the line W becomes the finishing point F. The circle C_R and C'_R is maximised when the circle C_P is inscribed in the circle C'_R. Thus, the circle C_R and C'_R are determined simultaneously and the desired avoidance trajectory is drawn as the curve OSF.

In this case, since half of the lateral displacement of avoidance is made by the former arc with the angle θ_B as shown in Figure 3(b), the following equation must be satisfied:

$$R_B - R_B\cos\theta_B = \frac{L_{Wr} - r}{2}. \tag{5}$$

Next, since the circle C_P is inscribed in the circle C'_R, the following equation must be satisfied:

$$R_B - r = \sqrt{(2R_B\sin\theta_B - x_{pr})^2 + (R_B + r - L_{Wr} - y_{pr})^2}. \tag{6}$$

The turning radius R_B is obtained by solving Equations (5) and (6) as follows:

$$R_B = \frac{-a_3 + \sqrt{a_3^2 - 4a_1^2 a_4}}{2a_1^2}, \tag{7}$$

where a_1, a_2, a_3 and a_4 are expressed as

$$a_1 = \frac{L_{Wr} - y_{pr}}{2x_{pr}}, \tag{8}$$

$$a_2 = \frac{x_{pr}^2 + y_{pr}^2 - r^2 + 2(L_{Wr} - r)y_{pr}}{4x_{pr}}, \tag{9}$$

$$a_3 = 2a_1 a_2 - L_{Wr} + r, \tag{10}$$

$$a_4 = a_2^2 + \frac{(L_{Wr} - r)^2}{4}. \tag{11}$$

The turning angle θ_B is derived from Equation (5) as follows:

$$\theta_B = \cos^{-1}\left(1 - \frac{L_{Wr} - r}{2R_B}\right). \tag{12}$$

Thus, the turning radius and turning angle of Steering B can be determined by Equations (7) and (12).

4. Autonomous collision avoidance system design

4.1. *Outline of the proposed system*

Figure 4 shows the flow of the proposed system which enables autonomous avoidance of a moving obstacle. This system consists of four subsystems. The following subsections describe them in detail.

4.2. *Surroundings recognition*

This subsystem recognises the road boundaries and the obstacle from the LIDAR data under the situation shown in Figure 1. This section describes the recognition method.

First, the ego-vehicle's position in the absolute coordinate system is calculated from the data obtained by the vehicle speed sensor and the yaw rate sensor. Next, the LIDAR data are converted into the absolute coordinate by considering the ego-vehicle's absolute coordinate, since the LIDAR data contain information of relative distance and angle from the ego-vehicle to a certain object. Thus, the position of ego-vehicle and the LIDAR data are obtained in the absolute coordinate system. Figure 5 shows an example of surroundings' recognition. The

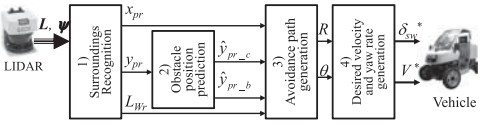

Figure 4. Outline of the proposed system.

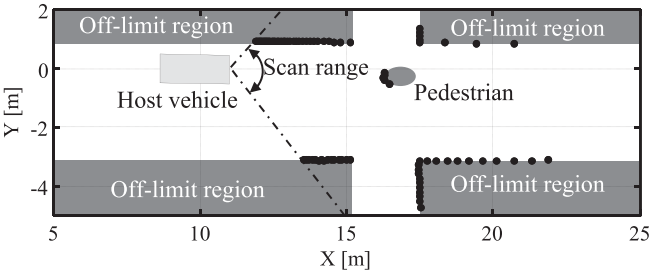

Figure 5. Scanned data by LIDAR.

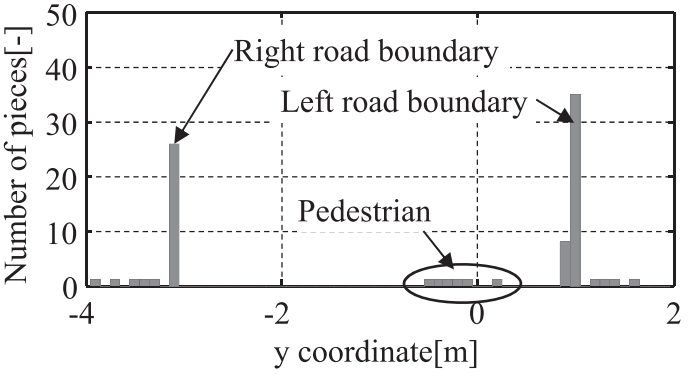

Figure 6. Distribution of the Y-coordinate.

LIDAR data shown by black dots, as well as the identified real road boundary and pedestrian are shown simultaneously for reference.

Figure 6 shows the distribution of the Y coordinates of LIDAR data cloud point in the absolute coordinate system. When the ego-vehicle is driven parallel to the road boundaries, the distribution forms two distinct peaks as shown in Figure 5. Hence, the Y coordinates of right and left road boundaries (L_{Wl} and L_{Wr}) can be obtained as the positive and negative mode values of the distribution.

In addition, if any LIDAR data exist within the road boundaries, they can be regarded as an obstacle. Then, the X and Y coordinate of the right corner of the obstacle x_{pr} and y_{pr} are obtained as the minimum data among the LIDAR data within the road boundaries, respectively. By similarly obtaining the coordinates of the left corner of the obstacle, the width of the obstacle w_0 can be obtained from the difference of the Y coordinates between the right and left corners of the obstacle.

Figure 7 shows an example of L_{Wl}, L_{Wr}, x_{pr} and y_{pr} acquired from the LIDAR data under the supposed environment by the method described above. The obtained LIDAR data are also shown. Figure 7 indicates that the proposed data-processing method can recognise the road boundaries and the obstacle properly.

4.3. *Obstacle position prediction*

This section describes the calculation method of the predicted position of the obstacle at the time instant when the ego-vehicle collides with the obstacle. This is done by predicting the

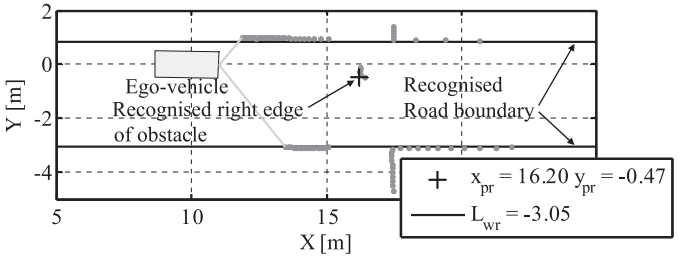

Figure 7. Result of surroundings recognition.

motion of the obstacle from the time history data of the right corner of the obstacle x_{pr} and y_{pr} obtained with the method described in the previous section.

The prediction is conducted only for the Y direction since this study supposes the situations that an obstacle crosses the road perpendicularly to the ego-vehicle.

The proposed subsystem assumes that the obstacle continues moving with a constant velocity and predicts its future positions with first-order prediction. The velocity of the obstacle v_{pr1} is calculated from the time history data of y_{pr}, as the difference of y_{pr} between at the time instant when an obstacle is recognised, t_0, and at a certain time instant, t_1 (later than t_0). The mathematical equation is expressed as follows:

$$v_{\mathrm{pr1}} = \frac{y_{\mathrm{pr}}(t_1) - y_{\mathrm{pr}}(t_0)}{t_1 - t_0}, \tag{13}$$

In this system, the motion prediction of the obstacle is conducted only once at the time t_1. t_1 is heuristically decided as the time 0.2 s later than t_0. The following calculation process is conducted at the time instant t_1. (Suffix '1' on the variables indicates that it is the value at the time t_1.)

The obstacle position at the time instant when the ego-vehicle collides with it is predicted with the obstacle's velocity expressed by Equation (13). Since the time for ego-vehicle to reach the expected collision location varies depending on whether the ego-vehicle brakes or not, two types of the obstacle position are predicted.

Here, two types of TTC are calculated. One is $T_{\mathrm{to\_c}}$ for the case that the ego-vehicle drives at an unchanged constant velocity and the other is $T_{\mathrm{to\_b}}$ for the case that it decelerates with maximum deceleration a_x. These are expressed as follows:

$$T_{\mathrm{to\_c}} = \frac{x_{\mathrm{pr1}} - X_{\mathrm{car1}} - l_{\mathrm{h}}}{V_1}, \tag{14}$$

$$T_{\mathrm{to\_b}} = \frac{-V_1 + \sqrt{V_1^2 + 2a_x(x_{\mathrm{pr1}} - X_{\mathrm{car1}} - l_{\mathrm{h}})}}{a_x}, \tag{15}$$

where X_{car1} and x_{pr1} indicate X coordinates of the ego-vehicle and the obstacle at the time instant t_1, respectively, V_1 is the velocity of the ego-vehicle at the time instant t_1, l_{h} the distance between the centre of gravity and the front end of the ego-vehicle and a_x the acceleration of the ego-vehicle. In this study, a_x is set to $-2\,\mathrm{m/s^2}$, the maximum deceleration which the experimental vehicle can generate by the in-wheel motors. To precisely calculate the prediction time in cases with steering, the effect of cornering must be considered in these equations. However, this effect is neglected in this study since the change of velocity in the X direction produced by steering is small enough against the distance between the ego-vehicle and the obstacle.

Using Equations (14) and (15), Y coordinates of the obstacle when the ego-vehicle reaches the obstacle's path are expressed as follows:

$$\hat{y}_{\mathrm{pr\_c}} = y_{\mathrm{pr1}} + v_{\mathrm{pr1}} \cdot T_{\mathrm{to\_c}}, \tag{16}$$

$$\hat{y}_{\mathrm{pr\_b}} = y_{\mathrm{pr1}} + v_{\mathrm{pr1}} \cdot T_{\mathrm{to\_b}}. \tag{17}$$

In the following section, $\hat{y}_{\mathrm{pr\_c}}$ is used for judgement of whether an intervention is necessary or not in a case that the detected obstacle is expected to move in on the ego-vehicle's path, whereas $\hat{y}_{\mathrm{pr\_b}}$ is for selection of the avoidance method and derivation of avoidance trajectory in a case that an intervention is decided to be necessary.

Preliminary experiments are carried out to verify the accuracy of a prediction. The results in detail are omitted in this paper. The results indicate that the proposed method predicts the future position of obstacles with average errors of five centimetres.

4.4. *Decision of avoidance method with generation of the avoidance trajectory*

This section describes the method for judging the necessity of an intervention and selecting an appropriate avoidance method if necessary. The derivation method of avoidance trajectory described in Section 3 is utilised to select an avoidance method. However, the radius r in Equations (1)–(12) is set to 0.8 m although the true half width of the vehicle is 0.5 m, in order to compensate for a prediction error of obstacle position and trajectory tracking error of the ego-vehicle.

Figure 8 shows the decision flow to select an appropriate avoidance method among the four defined in Section 3. In the proposed system, the priority is given to avoidance by braking rather than avoidance by steering because avoidance by braking has less influence on other vehicles in traffic. Thus, the availability of each avoidance method is assessed in sequence from avoidance by braking. This decision is made just once at the time instant t_1.

4.4.1. *Judgement of the necessity of autonomous avoidance*

The system executes an autonomous avoidance if TTC with the obstacle is less than 2 s. This is because the drivers generally complete avoidance behaviour before TTC becomes less than

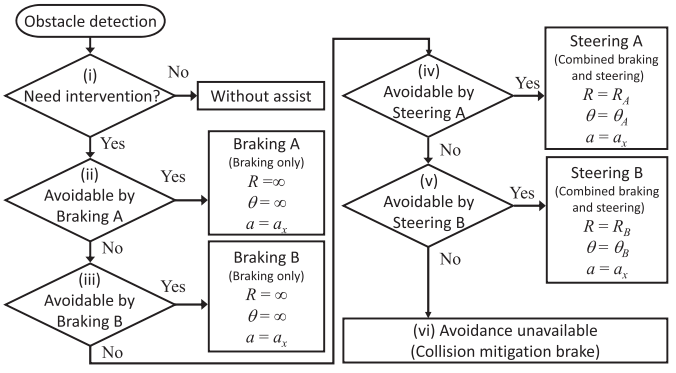

Figure 8. Decision rules of collision avoidance method.

2 s [8]. This is expressed as follows:

$$T_{\text{to\_c}} \leq 2, \tag{18}$$

$$-\frac{w_{\text{v}}}{2} - w_{\text{o}} < \hat{y}_{\text{pr\_c}} < \frac{w_{\text{v}}}{2}, \tag{19}$$

where w_{v} indicates the vehicle width, w_{o} indicates the width of the obstacle. When both of these inequalities are satisfied simultaneously, the system decides to conduct an evasive action.

4.4.2. *Judgement of availability of Braking A*

If an evasive action is decided to be conducted, the system first assesses the availability of Braking A, which makes the ego-vehicle stop before the obstacle. Braking A is available if the distance between the obstacle and the front end of the vehicle is more than the stopping distance of the ego-vehicle D as shown by the following inequality:

$$x_{\text{pr1}} - l_{\text{h}} \geq D \quad \left(= -\frac{V_1^2}{2a_x}\right). \tag{20}$$

If this inequality is satisfied, collision avoidance is available only by braking. Then the system outputs $R = \infty$ and $\theta = \infty$ as the command turning radius and turning angle, as well as the command acceleration $a = a_x$ to brake the ego-vehicle with maximum deceleration.

4.4.3. *Judgement of availability of Braking B*

If Braking A is not available, then the availability of Braking B, which allows the obstacle finish crossing before the ego-vehicle reaches the obstacle's path, is assessed. Braking B is available if the predicted obstacle position after $T_{\text{to\_b}}$ is out of the ego-vehicle's path, as shown by the following inequality:

$$\hat{y}_{\text{pr\_b}} < -\frac{w_{\text{v}}}{2} - w_{\text{o}}. \tag{21}$$

If this inequality is satisfied, collision avoidance is also available only by braking. Then the system outputs $R = \infty$, $\theta = \infty$ and $a = a_x$ as the command turning radius, turning angle and acceleration, as is the case in Braking A.

4.4.4. *Judgement of availability of Steering A*

If both of the avoidance methods by braking are not available, the system then assesses the availability of Steering A, which is an evasive action by steering without consideration of the presence of right road boundary. The turning radius R_{A} and angle θ_{A} calculated by substituting $x_{\text{pr}} = x_{\text{pr1}}$, $y_{\text{pr}} = \hat{y}_{\text{pr\_b}}$ and $L_{\text{Wr}} = L_{\text{Wr1}}$ into Equations (2) and (4) are used to assess the availability. Then, Steering A is available if turning with radius R_{A} does not make the ego-vehicle collide with the right road boundary. Moreover, the radius R_{A} must not be smaller than the minimum turning radius of the vehicle R_{min}. These conditions are expressed mathematically as follows:

$$L_{\text{Wr1}} \geq 2R_{\text{A}}(1 - \cos\theta_{\text{A}}) + r, \tag{22}$$

$$R_{\text{A}} \geq R_{\text{min}}. \tag{23}$$

If these inequalities are satisfied, Steering A is available. Then the system outputs the turning radius and angle to be conducted as $R = R_{\text{A}}$, $\theta = \theta_{\text{A}}$. In addition, at the same time, the

command acceleration is also output as $a = a_x$ (maximum deceleration) to stop the vehicle as soon as possible, because the supposed scenes are emergency avoidance scenes.

4.4.5. *Judgement of availability of Steering B*

If Steering A is not available, the system lastly assesses the availability of Steering B, which does consider the presence of right road boundary in the evasive steering. Similar to the assessment of Steering A, turning radius R_{B} and angle θ_{B} are first calculated by substituting $x_{\mathrm{pr}} = x_{\mathrm{pr1}}, y_{\mathrm{pr}} = \hat{y}_{\mathrm{pr\_b}}$ and $L_{\mathrm{Wr}} = L_{\mathrm{Wr1}}$ into Equations (7)–(12). Steering B is available if only the gap between the obstacle and the right road boundary is larger than the ego-vehicle's width. However, the radius R_{B} must not be smaller than the minimum turning radius of the vehicle R_{min}. These conditions are expressed mathematically as below:

$$L_{\mathrm{Wr1}} \geq 2r - \hat{y}_{\mathrm{pr\_b}}, \tag{24}$$

$$R_{\mathrm{B}} \geq R_{\mathrm{min}}. \tag{25}$$

Note that if L_{Wr} is wider than $2r + w_{\mathrm{o}} + w_{\mathrm{v}}/2$, the lower limit of Inequality (24) is covered by the Inequality (21) and therefore Inequality (24) is always satisfied logically. If these inequalities are satisfied, Steering B is available. Then the system selects Steering B, to output the turning radius and angle to be conducted as $R = R_{\mathrm{B}}, \theta = \theta_{\mathrm{B}}$. At the same time, the command acceleration of $a = a_x$ is output, as is the case in Steering A.

4.4.6. *Case of unavoidable collision.*

If all of the avoidance methods are judged to be unavailable, it means that collision with the obstacle is physically unavoidable. In this case, the system executes a collision mitigation brake with maximum deceleration without any steering.

4.4.7. *Theoretical coverage by the proposed decision rule*

Figures 9(b) and 10(b) show the conditions of the obstacle covered by each avoidance method in the case that the ego-vehicle is running on the left side of a road that is 3 and 4 m wide, respectively. The obstacle is assumed to be a pedestrian appearing from the roadside and to be detected at 0.1 m inside from the left road boundary. Then the values of parameters were set as shown in Figures 9(a) and 10(a), respectively. Figure 9(b) indicates that there exists a region where an avoidance method is not available between areas of Steering B and Braking B in the case of narrow road. Since this area means that the obstacle blocks the path of the ego-vehicle to leave no space for the ego-vehicle to pass through, avoidance of the obstacle is physically unavailable. Except for that region, most of the conditions are covered by the proposed avoidance methods. Figure 10(b) indicates that, in the case of wider road, the region where any avoidance methods are not available disappears between the regions of Steering B and Braking B because L_{Wr} is long enough and any condition of the obstacle under 4 m/s is avoidable by the proposed methods.

Considering that the obstacle is a pedestrian whose speed is 1 m/s, Figures 9 and 10 indicate that the system sufficiently covers the condition of pedestrians jumping out from the roadside and is useful in pedestrian collision avoidance.

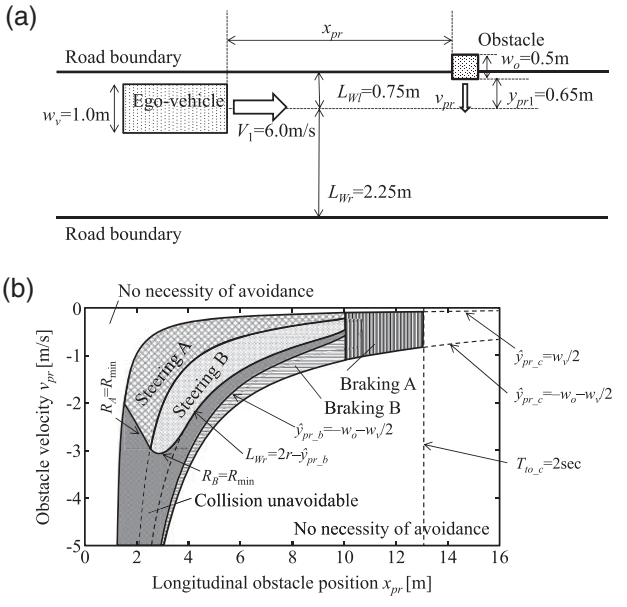

Figure 9. Theoretical coverage (on narrower road). (a) Values of parameters and (b) covered conditions.

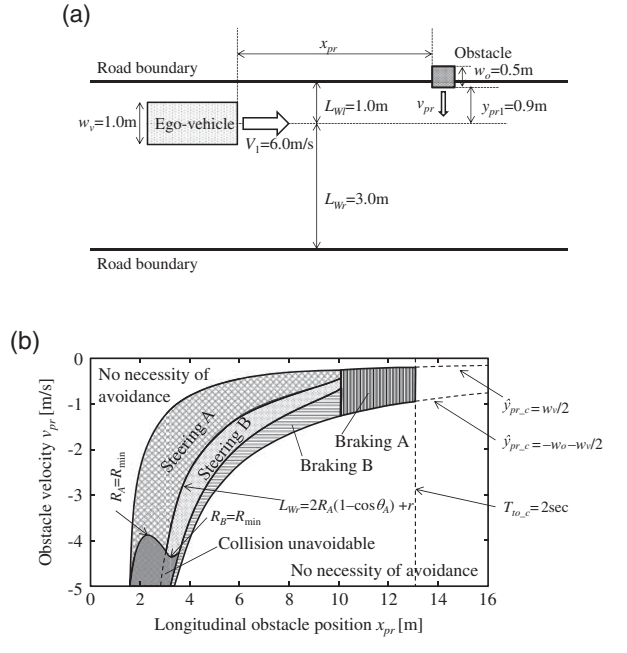

Figure 10. Theoretical coverage (on wider road). (a) Values of parameters and (b) covered conditions.

4.4.8. *Possibility of a side collision*

Since the system conducts an evasive action from the obstacle's position at the time instant when the front end of the ego-vehicle reaches the obstacle's path, there is a possibility for the obstacle to collide with the side of the ego-vehicle if it continues moving after that. However,

this paper defines this as 'collision avoided', because the system can prevent the vehicle from hitting the obstacle with its front end.

4.5. *Generation of the desired vehicle velocity and steering angle*

Tuning radius R and angle θ of the avoidance trajectory and command acceleration a are determined by the decision method described in the previous section. This section describes the method for generating the profile of the desired vehicle speed $V^*(t)$ and the desired steering angle $\delta^*_{\mathrm{sw}}(t)$ from the R, θ and a.

In this study, for any avoidance method, the system commands the maximum deceleration because the supposed scenes are emergency avoidance scenes. Therefore, in any case, the desired velocity $V^*(t)$ after the time t_1 is expressed as follows:

$$V^*(t) = \begin{cases} V_1 + a \cdot (t - t_1) & \text{if} \quad t_1 \le t \le \dfrac{V_1}{-a} + t_1, \\ 0 & \text{if} \quad t \ge \dfrac{V_1}{-a} + t_1, \end{cases} \tag{26}$$

where t indicates time.

The desired steering angle $\delta^*_{\mathrm{sw}}(t)$ is calculated from the turning radius R and angle θ output from the subsystem described in Section 4.4 by using Equation (27), which is derived from the ego-vehicle's characteristics in steady-state cornering.

$$\delta^*_{sw}(t) = \begin{cases} -\{1 + K(V(t))^2\} N \cdot \dfrac{l}{R} & (t_1 \le t < t_S), \\ \{1 + K(V(t))^2\} N \cdot \dfrac{l}{R} & (t_S \le t \le t_F), \end{cases} \tag{27}$$

where K indicates the stability factor, N the steering gear ratio, l the wheel base, t_{S} the steering switching time, t_{F} the finishing time of avoidance. t_{S} and t_{F} are expressed as follows:

$$t_{\mathrm{S}} = t_1 + \frac{V_1 - \sqrt{V_1^2 + 2aR\theta}}{-a}, \tag{28}$$

$$t_{\mathrm{F}} = t_1 + \frac{V_1 - \sqrt{V_1^2 + 4aR\theta}}{-a}. \tag{29}$$

Figure 11 shows the time history of the desired velocity $V^*(t)$ and the desired steering angle $\delta^*_{\mathrm{sw}}(t)$.

The autonomous avoidance is executed by inputting these $V^*(t)$ and $\delta^*_{\mathrm{sw}}(t)$ into the vehicle control DSP on the experimental vehicle.

5. Experiments

The experiments are carried out to verify the effectiveness of the proposed system with the experimental vehicle equipped with the proposed system. The road boundary and the obstacle were emulated by cardboard boxes for safety reasons. The cardboard box as the obstacle is 54 cm wide and 38 cm long. This cardboard box is pulled into the ego-vehicle's path via string from the roadside. Figure 12 shows a scene of the experiments.

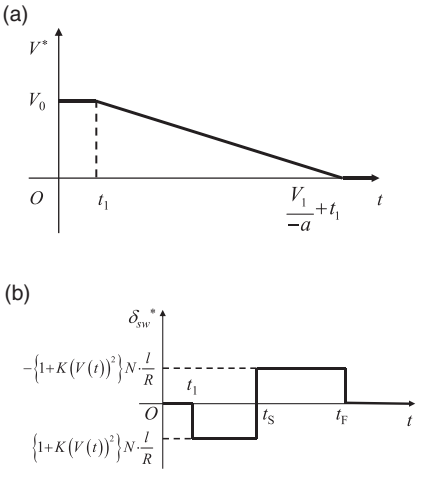

Figure 11. Time history of the desired velocity and steering angle. (a) Desired vehicle velocity and (b) desired steering angle.

Figure 12. A scene of the experiments.

Four representative results are shown in Figures 13–16, and the experimental conditions are shown in Table 1. In each figure, (a) shows the recognised surroundings, obstacle and vehicle trajectory. The origin is the vehicle's centre of gravity at the time when the system recognised the obstacle t_0. Among the trajectories, the grey broken line shows the desired trajectory, while the black solid line shows the actual trajectory. Each (b) shows the time history of the vehicle velocity (upper left), the steering angle (lower left) and the X and Y coordinates of the obstacle obtained from the LIDAR data (upper right and lower right, respectively). The origin of the time is when the system recognised the obstacle t_0.

Figure 13 shows the result where 'Braking A' was selected. In this condition, although an intervention is needed, the distance to the obstacle was relatively long. Therefore, the system judged that the ego-vehicle can stop before the obstacle, and avoided collision by braking without steering.

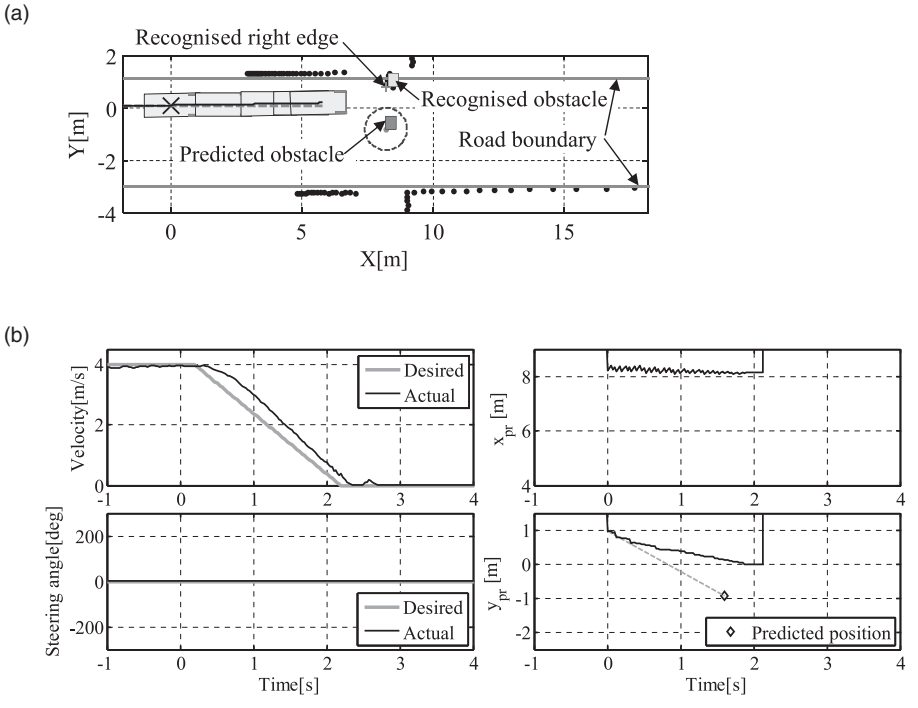

Figure 13. Experimental result (condition 1). (a) Vehicle trajectory and (b) time history of ego-vehicle and obstacle.

Figure 14 shows the result where 'Braking B' was selected. In this condition, an intervention was needed and it was impossible to stop before the obstacle. However, since the velocity of the obstacle was high, the system judged that it is possible to let the obstacle finish crossing the ego-vehicle's path by braking without colliding. Then, the collision was avoided by braking without steering.

Figure 15 shows the result where 'Steering A' was selected. In this condition, it was impossible to avoid collision only by braking. However, because the ego-vehicle's velocity was relatively high, the predicted obstacle position was near the left road boundary and therefore a large lateral displacement was not needed to evade the obstacle. For this reason, the system selected 'Steering A' which does not consider the right road boundary, and avoided collision by appropriate steering with braking.

Figure 16 shows the result where 'Steering B' was selected. In this condition, it was impossible to avoid collision only by braking, and relatively large lateral displacement was needed because the predicted obstacle position was far from the left road boundary. Therefore, it was necessary to consider the presence of the right road boundary. Thus, the system selected 'Steering B' which takes the right road boundary into account, and avoided collision by appropriate steering with braking.

From these experimental results, it is indicated that the system can avoid collision with a moving obstacle, leading to the conclusion that the proposed system is effective. However, some challenges below are revealed.

Figures 15(a) and 16(a) indicate that the ego-vehicle cannot follow the desired trajectory and causes errors in lateral displacement. This is because the actual steering angle does not follow the desired steering angle at the start of steering, as indicated by lower left graphs in Figures 15(b) and 16(b), which show the time histories of the steering angle. This tracking delay is caused by the limitation of rotation speed of the servomotor (500 deg/s). In this

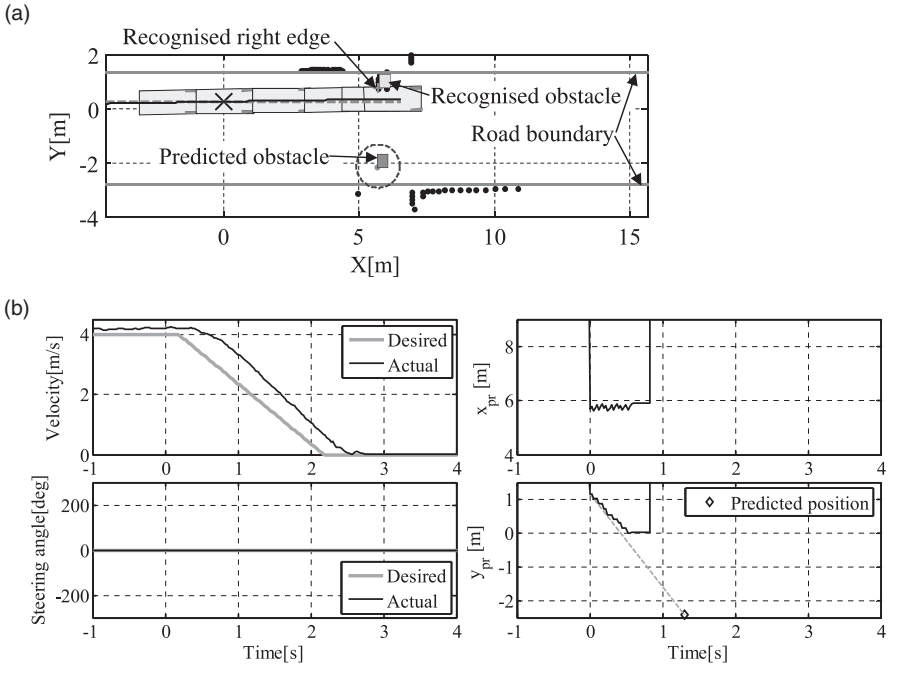

Figure 14. Experimental result (condition 2). (a) Vehicle trajectory and (b) time history of ego-vehicle and obstacle.

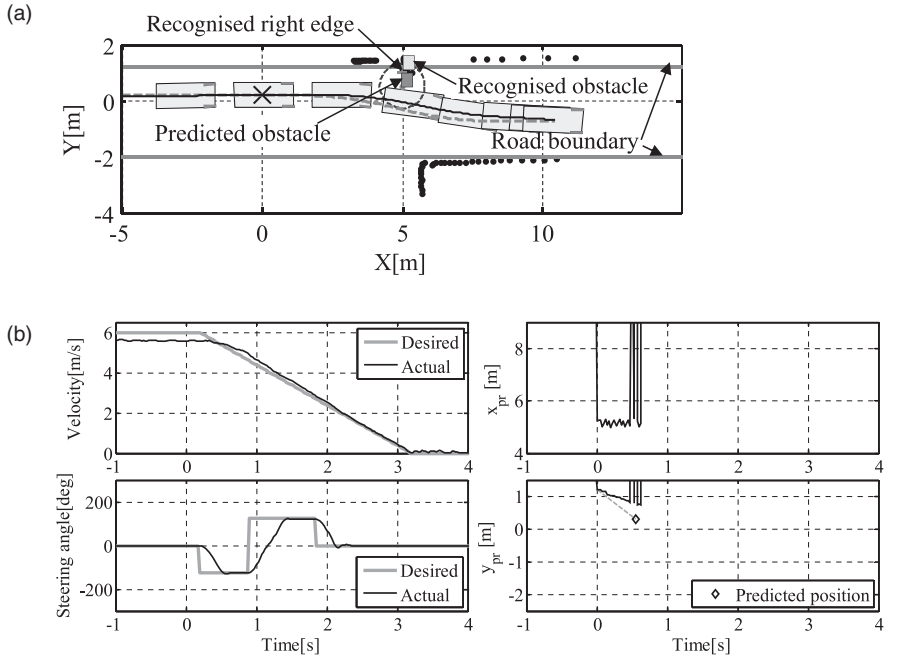

Figure 15. Experimental result (condition 3). (a) Vehicle trajectory and (b) time history of ego-vehicle and obstacle.

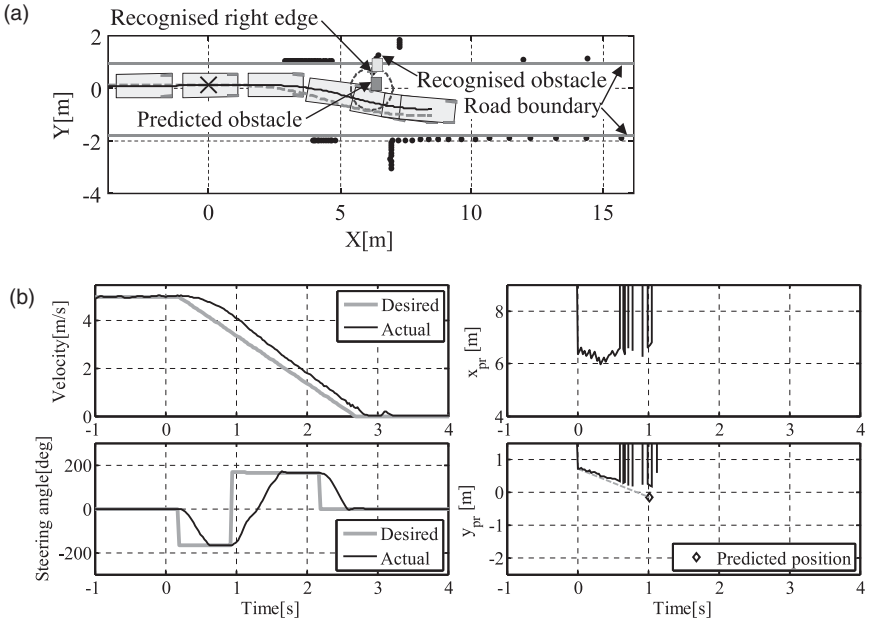

Figure 16. Experimental result (condition 4). (a) Vehicle trajectory and (b) time history of ego-vehicle and obstacle.

Table 1. Experimental conditions.

No.	V_1 (m/s)	x_{pr1} (m)	v_{pr1} (m/s)	L_{Wr1} (m)	Decision
1	3.97	8.18	1.00	3.09	Braking A
2	4.20	5.61	2.19	3.15	Braking B
3	5.58	5.19	0.90	2.10	Steering A
4	5.00	6.32	0.63	1.90	Steering B

study, an extra margin of 0.3 m is added in the radius r drawn centred on the right edge of the obstacle, in order to compensate the tracking error caused by the limitation of rotation speed. Therefore, collision avoidance is achieved even with this tracking error. However, for precise assessment of the availability of the avoidance, it is an important challenge to derive the avoidance trajectory by considering the limitation of the steering system.

The other challenge revealed is concerned with the motion prediction. The time history graphs of the obstacle position, which are shown by the right graphs in Figures 13(b)–16(b), indicate that the system misses the obstacle at 0.5–2.0 s after detecting it. This is because the ego-vehicle is too close to the obstacle to recognise the obstacle and road boundaries or the turning motion of the ego-vehicle excludes the obstacle from the scan area of the LIDAR. In Figures 14–16, the predicted positions of the obstacles agree with the recognised actual motions. However, in Figure 13, an error of approximately 1 m is observed between the predicted and actual position of the obstacle. This is caused by a deceleration of the obstacle after recognition. Since real pedestrians are likely to change their motion, decelerate or accelerate, after starting to cross roads, the system must be improved to respond to the change of motion of the obstacle from a practical viewpoint.

6. Conclusions

This paper proposed an autonomous collision avoidance system that can evade obstacles jumping out from the side of the road based on constant-velocity obstacle motion prediction. The proposed system is designed to recognise the road boundaries and the obstacle by a LIDAR, predict the future position of the obstacle, derive a geometrically optimised avoidance trajectory, select the most appropriate avoidance method and conduct autonomous avoidance with combined control of steering and braking. Autonomous collision avoidance by the proposed system was successfully conducted in the demonstration experiments, and the effectiveness of the proposed system was verified by experiments using actual vehicle.

Acknowledgements

This work was partly supported by the Grant-in-Aid for Young Scientists (B) (23760201), JSPS.

References

[1] Institute of Traffic Accident Research and Data Analysis, *Analysis of human factors in crossing collisions*, ITARDA information, No. 56 (2005). Available at http://www.itarda.or.jp/itardainfomation/english/info56/56top.html.

[2] M. Shimizu, M. Usami, and H. Fujinami, *Development of Collision-Avoidance Assist System* (2007 JSAE Autumn Convention) Proceedings, No. 148-07, 2007, pp. 25–30.

[3] T. Wakazuki, *Study on brake-control timing of forward collision avoidance assistance systems*, JARI Res. J. 27(10) (2005), pp. 594–597.

[4] S. Horiuchi, R. Hirao, K. Kazuyuki, and S. Nohtomi, *Optimal steering and braking control in emergency obstacle avoidance*, Trans. Jpn. Soc. Mech. Eng. Ser. C 72–722(06–0356) (2006), pp. 180–185.

[5] T. Fujioka, A. Shibata, Y. Tsukasaki, and S. Sawada, *Vehicle motion control for minimizing collision risk by use of optimal control theory* (2008 JSAE Spring Convention) Proceedings, No. 8-08, 2008, pp. 21–26.

[6] A. Ohmuro, and Y. Hattori, *Optimum vehicle trajectory control for obstacle avoidance – a minimax problem of resultant vehicle force*, Trans. Jpn. Soc. Mech. Eng. Ser. C, 76(772) (2010), pp. 3587–3594.

[7] R. Hayashi, J. Isogai, S. Fujita, P. Raksincharoensak, and M. Nagai, *Development of autonomous forward obstacle avoidance system by using in-wheel-motor and steering control of micro electric vehicle*, JSAE Trans. 42(1) (2011), pp. 87–93.

[8] K. Matsubayashi, Y. Yamada, and M. Iyoda, *Development of rear pre-crash safety system for rear-end collisions*, TOYOTA Tech. Rev. 55(1) (2006), pp. 84–89.